Analysis of Scour under Vertical Circular Jet using Sand-Gravel Mixture Sediment

[1]Gopal Malba Alapure
Dhole Patil College of Engineering, Pune, Maharashtra,India

Corresponding Author-[1]Gopal Malba Alapure
Dhole Patil College of Engineering, Pune, Maharashtra, India

[2]Pradeep Rana
National Institute of Technology Kurukshetra, India

[3]Bharat Murlidhar Shinde
Bharat College of Engineering, Badlapur(W), Thane, Maharashtra,India
bharat_mshinde@yahoo.co.in

[4]Vikas Singh

Abstract:
Scour is a very limited erosion of ground material brought on by water jets impinging on downstream water. The ultimate bed scour hole is produced by static scour, which happens when jet flow has halted, and dynamic scour, which happens while jet flow is active. Designing downstream protection measures requires an accurate estimation of the scouring character. The depth of scouring formed by water jets is influenced by interdependent factors such as velocity, jet height, nozzle size, and sediment characteristics. This study completed 36 tests on an iron tank at various impinging heights and velocity ranges. The scour bed was composed of 50:50 locally accessible sand and gravel with sedimentary characteristics. Under static circumstances, a pointer gauge was used to record of the scour holes geometry, the dune height, and the associated scour factors. On the basis of the observed data, the scour hole volume, and erosion parameters (Ec) were calculated.

Keywords: Vertical Circular Jet, Sand-Gravel Mixture Sediment, Depth of scouring, Scour Hole Radius, Dune height, and Volume of Scour Hole

Introduction:

Growing issues in the river system include unsteadiness and hydrodynamic imbalance brought on by both natural and artificial forces. Depth of scour around hydraulic projects is critical to their stability, including spur dikes, jets, abutments, and bridges. An significant rise in depth puts the foundation's stability at peril. Accordingly, estimating the highest scouring depth that water jets might create is essential for constructing hydraulic structures safe and economical. The research study of the scouring process induced by jets of various sizes and features rekindles interest in the comprehension of the scour process. When turbulent flow fields interact with erodible bed sediments downstream of hydraulic structures, a complex phenomenon known as scour is created by the water jets. Scour adds another layer of complication when solid sediment is mixed in. Scour created by submerged water jets occurs under hydraulic structures such free overfall spillways and trajectory bucket type energy dissipators. Sprays of water that shoot out of the hydraulic structures and press on the water downstream generate scour around the structures.

It's critical to evaluate features such maximum scour depth, outlet diameter, and jet height beneath submerged jets while constructing protective measures downstream of the structures. Developing methods to control and guide the scour process is necessary for designers to

lessen the risk of hydraulic structural collapse. Stirring jets are often connected to specified hydraulic components like permanent structures and mobile sources. When the water flow is strong, the shear pressures across the bed may become too high, which can cause the sediment bed to get seriously damaged in some places.

Litrature Review:

Circular jets may cause localized scouring in the vicinity of structures of hydraulics, endangering, structural integrity of such structures. The local scour process is complicated by significant fluctuations in flow characteristics over the erodible substrate. Submerged vertical circular water jets have four main flow zones: the wall jet, the impinging jet, the free jet, and maybe the core flow region.Two different forms of scour holes were reported by Westrich and Kobus (1973), depending on the value of Ko, which is specified by equation 1 below. The experiment used a vertical submerged water jet with a nozzle diameter of 20 mm to 40 mm and a velocity of jet 0.7 m/s to 3.7 m/s on a homogeneous sand substrate. For a particular set of jet parameters, the scouring hole volume enlarges with jet height, then remains constant before dropping once more. Rajaratnam, N. (1981) investigated erosion under plane turbulent wall jets in a laboratory setting and the research was divided into three series: the first involved scouring non-cohesive materials with plane turbulent air jets using a single nozzle with a thickness of do = 2.41 mm; the second involved scouring non-cohesive materials with plane turbulent air jets using the same nozzle; and the third involved fourteen equilibrium laboratory studies on the erosion of sand beds by submerged water jets in a rectangular test flume that was 5.5 m in length, 0.66 m in depth, and 0.31 m in width. By employing an octagonal plastic box with an impinging jet affixed to the bottom of a 150 mm diameter, Aderibigbe and Rajaratnam (1996) conducted laboratory investigations to identify the decisive impinging jet distance at which static depth of scour is large. It was feasible to anticipate the locations of no scour at hj equal to 505 mm (Ec = 0.18) and 790 mm (Ec = 0.14), respectively, by extrapolating the scour curves. For hj values higher than the critical value, the static and dynamic scour depths are almost the same. Rajaratnam and Mazurek (2003) conducted an experimental research study in the laboratory on scouring in non-cohesive soil under turbulent water jets with a restricted tail water level. They arrived at the conclusion that there are two different kinds of scouring: static and dynamic. They also concluded that during a large percentage of the scour, the maximum depth of scour grows linearly with logarithm of time until it achieves equilibrium conditions. They also mentioned that, under dynamic circumstances, the scour depth is three times more than it is under static conditions, or equilibrium conditions. Dey and Raikar (2007) investigated scouring in sand and gravels using a huge vertical drop. A 0.3 m by 0.7 m flume with a 0.5 m high vertical drop at one end was used for the investigations. The sediments used in the trial runs were sand and gravel. The six samples had mean diameters of 0.26, 0.49, 0.81, 1.86, 2.54, 3 mm, and 4.1, 5.53, and 7.15 mm. Ghodsian and Ranjbar (2012) examined scour caused by the free-falling jet by taking into account tailwater depth, Densimetric Froude number, drop height, and sediment size. They discovered that the jet splits into two parts upon striking the bed: one portion moves toward the downstream end (strong flow) and the other portion moves toward the upstream end (weak flow). The formation of an armor layer is found to explain the inverse relationship between the scouring hole and the geometric standard deviation of the sediment. The reaction of a gravel substrate to vertically operating, submerged water jets was investigated by Chakravarti, Jain, and Kothyari (2014).

The four parameters that were considered were the nozzle diameter, jet velocity, sediment size, and jet impinging height. Both dynamic and static environments were used to quantify erosion. Maleki and Fiorotto (2019) conducted research on high hydraulic structures to foresee the shape and depth of scour on the downstream end of rectangular falling jets. The

results showed that scouring was visible in two places: the wall jet region and the impingement zone. Kartal and Emiroglu (2021) conducted experiments involving three nozzle diameters, two impingement lengths, and jet exit velocities and observed that nozzles with plates entrained more air bubbles into the impingement pool than jets without plates, reducing the maximum scour depth by spreading the scour over a larger area. Shakya et al. (2022) employed four impinging heights, a 1.62 cm diameter of nozzle diameter, and velocities of jets ranging from 1.57 m/s to 3.94 m/s in their investigations. Although the scour process in cohesiveless sediment under submerged water jets has been well investigated, little is known about the scour process in combinations of materials found in river beds, such as clay-gravel, and clay-sand-gravel combination. This study attemped to investigate the effects of scour resulting from differences in the jet's velocity, nozzle diameter, and impinging height in the presence of an uneven sediment bed.

Experimental Set-Up:

An iron tank measuring of 0.8 m x 0.8 m x 0.76 m of Hydraulics Laboratory of Department of the Civil Engineering, National Institute of Technology, Kurukshetra, served as the experimental setup. The water tank was modified with a valve to control the excess discharge at the bottom face. Throughout the trial runs, water was continually supplied via the galvanized iron pipes into an above tank with a 5720 liter capacity. The dimensions of the tank are 3.75 meters long, 1.25 meters wide and 1.22 meters high. The defining drawing of the jet with depth of scouring hole is shown in Figures 1a and 1b. Figure 2 displays the configuration image.

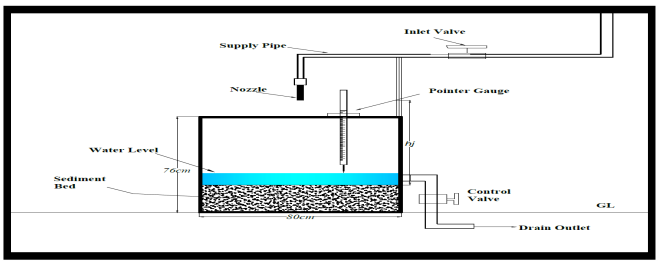

Figure 1a. Experimental Setup Line Diagram

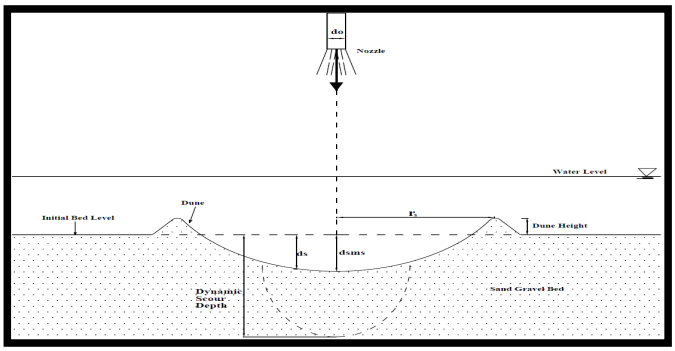

Figure 1b. Definition Sketch

Figure 2. Pictographic Views of Setup

Laboratory Parameters

Variations were made to the jet velocity, impinging height, nozzle diameters, constant run length, and fixed sediment size throughout the laboratory testing. The majority of the tests included changing the value of one parameter while leaving the values of the other parameters unchanged. The various parameter configurations used in the tests are explained in detail.

Jet Velocity

This is effectively the velocity at which the jet is projected from the nozzle tip. For the trials, four distinct velocities-1.50 m/s, 1.76 m/s, 2.76 m/s, and 3.76 m/s were used. Several runs were initially conducted for the same velocity value in order to achieve homogeneity in the experimental results.

Diameter of Nozzle

There were three nozzle diameters chosen: 25.4 mm, 19.05 mm, and 12.70 mm. Throughout testing, it was discovered that the nozzle's jet streams were turbulent. A pictorial representation of the nozzle diameters used in this study is shown in Figure 3. A nozzle with a diameter of 25.4 mm and three distinct lengths is shown in Figure 3(a). Additionally, Figure 3b shows a 12.7 mm nozzle diameter with three different lengths. Figure 3(c) shows a diameter of 19.07 mm. All of the modals are shown combined in Figure 3(d), and a sectional image of every nozzle is shown in Figure 3(e). Each pipe's length was chosen to provide the appropriate separation from the sediment bed's top (impinging height).

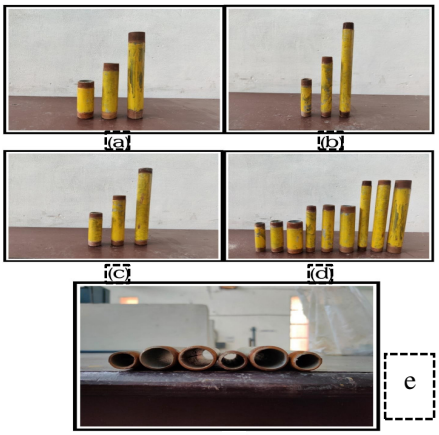

Figure 3. Nozzles used in experiment. (a) Nozzle dia.(do)=25.4 mm, (b) Nozzle dia.(do)=12.7 mm, (c) Nozzle dia.(do)=19.07 mm, (d) All nozzles in a view, (e) Sectional view of the nozzles.

Vertical Jet Impinging Height

The experiment involved a vertical distance between the sediment bed's top and the nozzle tip at jet impinging heights of 77.6 cm, 72.6 cm, and 65.6 cm, with three distinct nozzle lengths chosen to minimize misunderstandings and unnecessary measurements.

Sediment Size

The study examined sediment beds with equal proportions of sand and gravel. The particle size distributions of the utilized sediment were calculated using the Indian Standard Code (IS 1948-1970) methods for sand and gravel, as shown in Figures 4 and 5. Sand and gravel had geometric standard deviations (d50) of 1.73 and 1.31 mm, respectively, with corresponding sizes of 0.27 and 3.52 mm. The weighted arithmetic mean of the sand and gravel sizes was used to get the mean size of the sand-gravel combination. The mean sand-gravel size that was calculated was (d50a) = 1.90 mm. The silt had a relative density of 2.65. Images of gravel, sand, and a mixture of gravel and sand are shown in Figure 6.

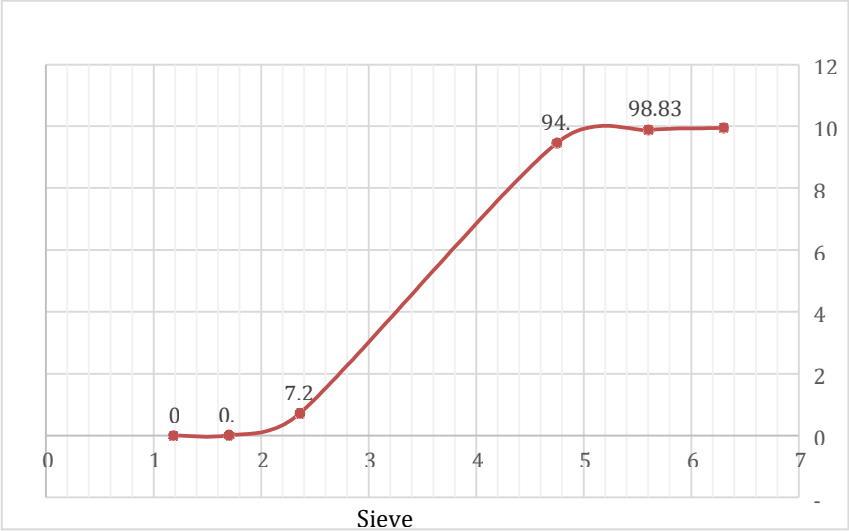

Figure 4. Particle Size Distribution Curve of Sand

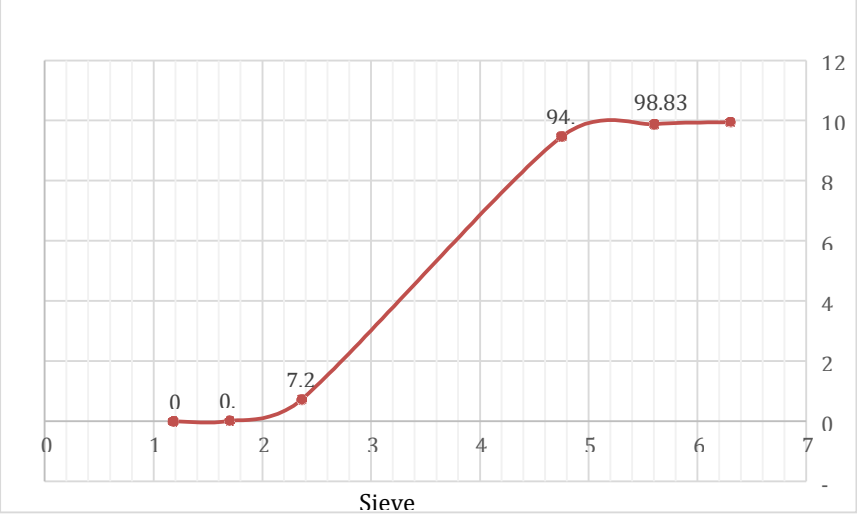

Figure 5. Distribution Curve of Gravel Particle Size

Table 3. Properties of Sediments

Sediments	Average sedimentsize, d_{50} (mm)	d_{85} (mm)	d_{16} (mm)	Geometric standard deviation(σg)	Specific gravity (G)
Sand	0.27	0.55	0.18	1.73	2.65
Gravel	3.52	4.48	2.6	1.31	2.65

Figure 6. Cohesionless Sediments. a) Sand (d_{50}) =0.27mm, b) Gravel (d_{50}) =3.52 mm, c) Sand Gravel mixture (d_{50a}) =1.907 mm

Experimental Methodology:

A 6.4 kg hammer and a 0.40 m long hardwood board were used to smooth and compress the top surface of the sediment bed. To prevent any inadvertent disruptions, every attempt was taken to guarantee that the top tank, which is used for the distribution of water, remained completely full throughout the testing runs. Once the trials at this height were finished, nozzle pipes of the same diameter and different lengths were used to test at higher impinging heights of 0.726 m and 0.756 m. Material was put into the tank at the lowest impinging height of 0.656 meters. Because of this, testing was conducted at three different jet impinging heights. To keep the tail water depth consistent at first, very little water was allowed to enter and remain on the sediment bed. Then, while the stopwatch was being set, a series of jet descents were permitted on the sediment bed, causing scour. The experiments were conducted for sixty minutes in order to achieve the equilibrium scour condition. The corresponding velocities for the nozzle diameters (19.07 mm, 12.70 mm, and 25.4 mm) that were used in the trials were 1.50 m/s, 1.76 m/s, 2.76 m/s, and 3.76 m/s. Using a simple point gauge that travelled around the tank's walls on an adjustable rail system, the static scour depth was determined to within 0.1 mm of accuracy. The water was allowed to flow out and the jet was turned off in order to assess the static scour depth without affecting the scour bed profile. Any excess water may be drained into the laboratory's subterranean sump channel via a hose connection aperture in the water tank's right wall. Table 2 presents the experimental plan.

Table 2 Scheme of Experimentation

Run No.	Velocity(m/s)	Weighted Mean sediment size (mm)	Impinging height (cm)	Nozzle diameter(mm)
SG01	1.50	1.90175	77.6	25.4
			72.6	25.4
			65.6	25.4
			77.6	19.07
			72.6	19.07
			65.6	19.07
			77.6	12.7
			72.6	12.7
			65.6	12.7
SG02	1.76	1.90175	77.6	25.4
			72.6	25.4
			65.6	25.4
			77.6	19.07
			72.6	19.07
			65.6	19.07
			77.6	12.7
			72.6	12.7
			65.6	12.7

SG03	2.76	1.90175	77.6	25.4
			72.6	25.4
			65.6	25.4
			77.6	19.07
			72.6	19.07
			65.6	19.07
			77.6	12.7
			72.6	12.7
			65.6	12.7

The vertical jet scour dataset was observed for four jet velocities, three jet heights, and constant sediment size in this experimental endeavor. The following variables were taken into account in the experiments: three jet diameters (25.4, 19.07 mm, and 12.7 mm), three impinging heights (0.77 m, 0.72 m, and 0.65 m), and four jet velocities (3.7 m/s, 2.76 m/s, 1.76 m/s, and 1.50 m/s). In a lab, the engineering characteristics of a mixture of equal parts sand and gravel material were ascertained.

Results and Discussion:

A circular vertical water jet was used to capture the scour data (36 permutations) throughout the course of an hour-long laboratory test. Additionally, a comparison was made between the acquired findings and those of earlier studies. In terms of the dune height, scour hole radius, scour hole volume, specific energy, and erosion parameter, the gathered scour data was evaluated.

Scour Parameters

The scour parameters-static scour depth, scour hole radius, dune height, and scour hole volume are discussed in the following paragraphs:

Scour Depth

The scour depth was measured using a pointer gauge that had a 0.1 mm precision. When the jet is turned off and the extra water is gently evacuated to prevent disturbing the bed profile, the scour depth is detected in a static state mode. By deducting the bed level information from the scour hole readings acquired from the point gauge, scour depths were computed. The equilibrium state was confirmed after 50–60 minutes when there was no discernible movement of the sediments.

Scour Radius

Bed level measurements were restricted to one diagonal in order to determine the overall scour hole geometry since the vertical circular jet created axis symmetric static scour hole profiles. In contrast, the radius of the scour hole was calculated by averaging two observations. Both the longitudinal and lateral orientations of the scour hole were utilized for these two measurements (highest value), and an estimate of the radius was made.

Volume of Scour Hole

The water replacement technique was used to determine the scour hole's volume. Using this approach, the quantity of water required to fill the scour hole to the fullest in the event of no seepage is calculated. Nevertheless, we also see the same scour hole’s volume values if we consider that the scour hole shape was parabolic and focussed, which were almost identical.

Dune Height

Dune height of scour hole was calculated by subtracting the point gauge readings at bed level from the readings at the top of the dune, using visual examination as the basis. To improve the accuracy of the dune height calculation, four measurements were averaged by keeping an eye on the scour levels.

Results of Experimental Study

The values of the dune height, scour hole volume, scour hole radius, and static scour depths based on three nozzle diameters, four jet velocities, and the jet's impinging height are shown in Table 3. These combinations, which go by the names SG01, SG02, SG03, and SG04, feature a mixed sediment bed and an hour-long continuous runtime.

Table 3. Data Collection for Final Scheme of Experiments.

Run No.	Velocity, v_o (m/s)	Nozzle Diameter, d_o (mm)	Impinging Height, h_j (cm)	Scour Depth, d_s (cm)	Scour Radius, r_s (cm)	Dune Height, Δs (cm)	Scour Hole Volume, ∇s (cm^3)
SG01	1.50	25.4	77.6	3.9	13.755	1.328	1158.47
		25.4	72.6	4.1	13.875	1.343	1239.22
		25.4	65.6	3.7	13.375	1.312	1039.18
		19.07	77.6	3.7	12.11	1.265	851.90
		19.07	72.6	3.9	12.757	1.279	996.46
		19.07	65.6	3.6	11.988	1.236	812.26
		12.7	77.6	3.1	12.233	1.129	728.33
		12.7	72.6	3.5	12.625	1.211	875.85
		12.7	65.6	3.4	11.575	1.097	715.19
SG02	1.76	25.4	77.6	4.7	11.757	1.623	1019.98
		25.4	72.6	4.9	15.252	1.645	1789.57
		25.4	65.6	4.6	15.075	1.543	1641.24
		19.07	77.6	4.2	14.352	1.452	1358.23
		19.07	72.6	4.5	14.89	1.471	1566.40
		19.07	65.6	4.4	14.757	1.414	1504.35
		12.7	77.6	3.9	13.233	1.321	1072.21
		12.7	72.6	4.2	13.797	1.382	1255.22
		12.7	65.6	3.8	14.111	1.333	1187.95
SG03	2.76	25.4	77.6	6.8	16.43	1.805	2881.93
		25.4	72.6	7.1	15.95	1.813	2835.82
		25.4	65.6	6.3	14.93	1.796	2204.75
		19.07	77.6	5.5	14.65	1.711	1853.27
		19.07	72.6	5.9	14.575	1.723	1967.74
		19.07	65.6	5.2	13.6	1.7	1510.01
		12.7	77.6	5.0	12.53	1.645	1232.46
		12.7	72.6	5.1	13.1	1.623	1374.08
		12.7	65.6	4.9	11.975	1.615	1103.18
SG04	3.76	25.4	77.6	9.9	19.75	2.175	6062.74
		25.4	72.6	10.3	20.375	2.165	6713.24
		25.4	65.6	9.7	19.325	2.075	5687.36
		19.07	77.6	7.6	19.25	1.825	4421.55
		19.07	72.6	8.3	19.425	1.925	4917.00
		19.07	65.6	7.7	19.85	1.823	4763.34
		12.7	77.6	7.2	19.88	1.721	4467.50
		12.7	72.6	7.6	20.525	1.692	5026.66
		12.7	65.6	7.1	20.27	1.655	4580.00

Following paragraphs will address the plotting and discussion of graphs with various parameters based on the data in Table 3.

Maximum Depth of Static Scour and its Relation to Impinging Height

Figures 7(a-d) illustrate the differences in static scour depths for three nozzle diameters throughout four sets of experiments with respect to impinging distance. These four graphs illustrate the critical impinging distance at which the greatest static scour depth is found. According to Aderibigbe (1996), the jet often breaks through the bed, enabling deteriorated material to exit the scour hole. Due to the deflected jet's restricted capacity to carry material over greater radial distances, deposition occurs on the inner walls of the scour hole, driving the deposited material toward the direction of the erosion center.

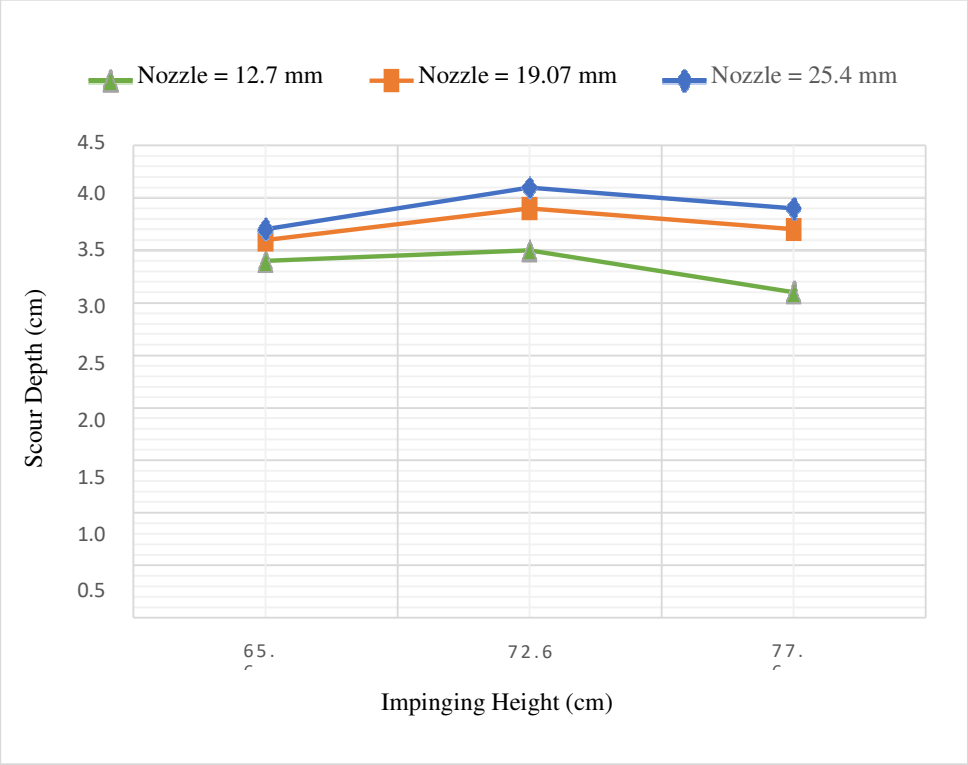

Figure 7a. Variations of scour depth with impinging height for jet velocity,(vo) =1.50m/s

Figure 7(a) shows how the static scour depth (ds) varies with impinging height based on three nozzle jet diameters (25.4 mm, 19.07 mm, and 12.7 mm) and a jet velocity (vo) of 1.50 m/s. For a given nozzle diameter, the maximum static scour depth decreases as the scour depth (ds) rises to 72.6 cm and the jet's impinging height (hj) rises. Figure 7(a) makes this very evident. Because the deflected jet can no longer carry material across longer radial distances, silts build up on the inner walls of the scour hole. The process of driving the deposited material to move toward the erosion center results in recurrent erosion. A similar trend has been seen for jet diameters of 25.4 mm and 19.07 mm as well. For velocities of 1.76, 2.76, and 3.76 m/s, other comparable graphs are also produced, as shown in figures 7(b), (c), and (d). However, when vo rises, the maximum static scour depth shows a similar pattern, as seen in Figures 7(a), (b), (c), and (d).

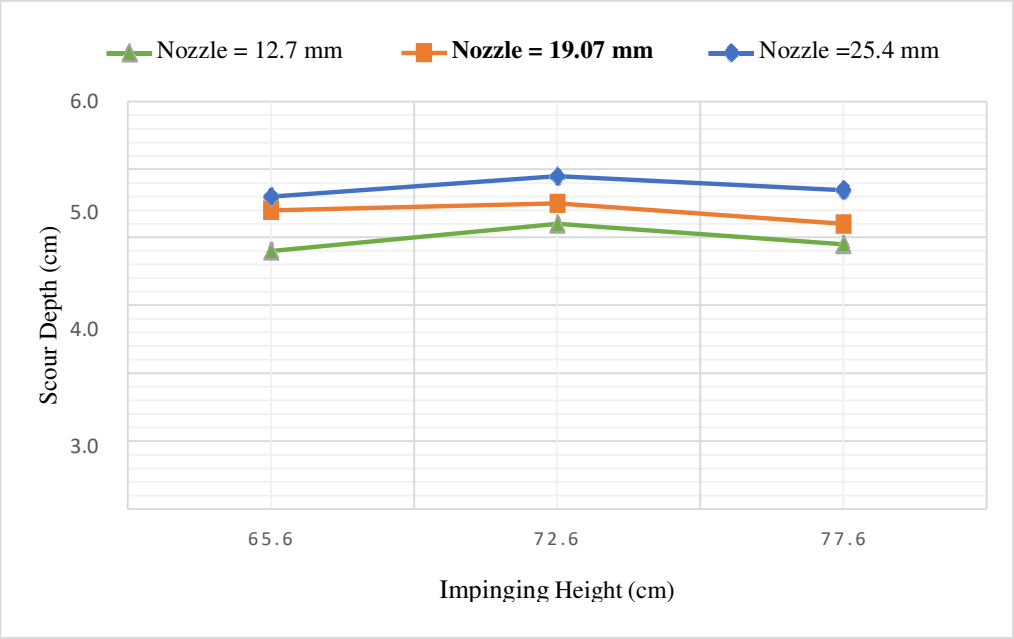

Figure 7b. Variations of scour depth with impinging height for jet velocity,(vo)=1.76m/s

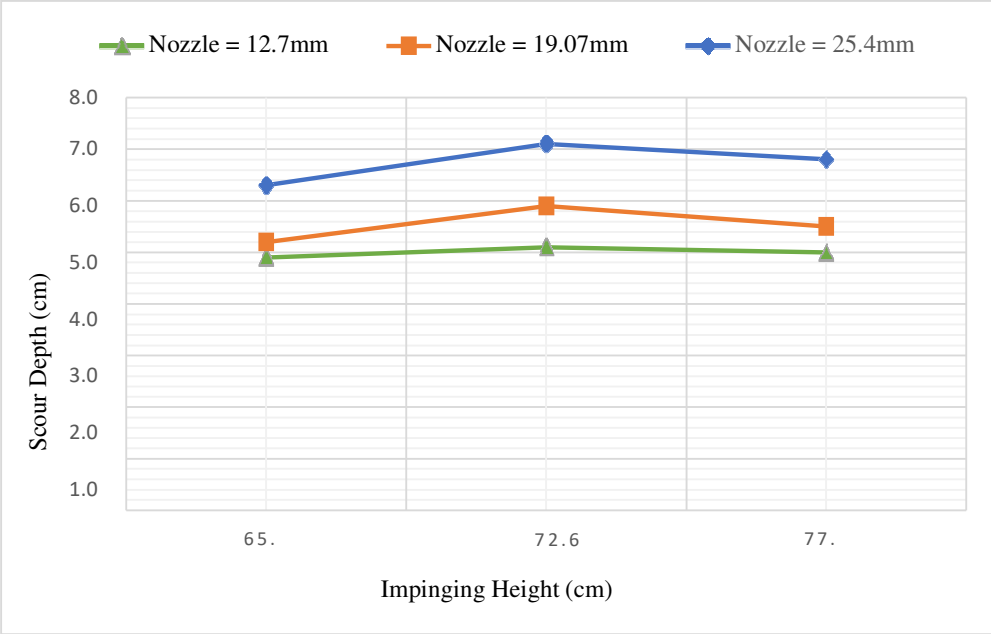

Figure 7c. Variations of scour depth with impinging height for jet velocity,(vo) = 2.76m/s

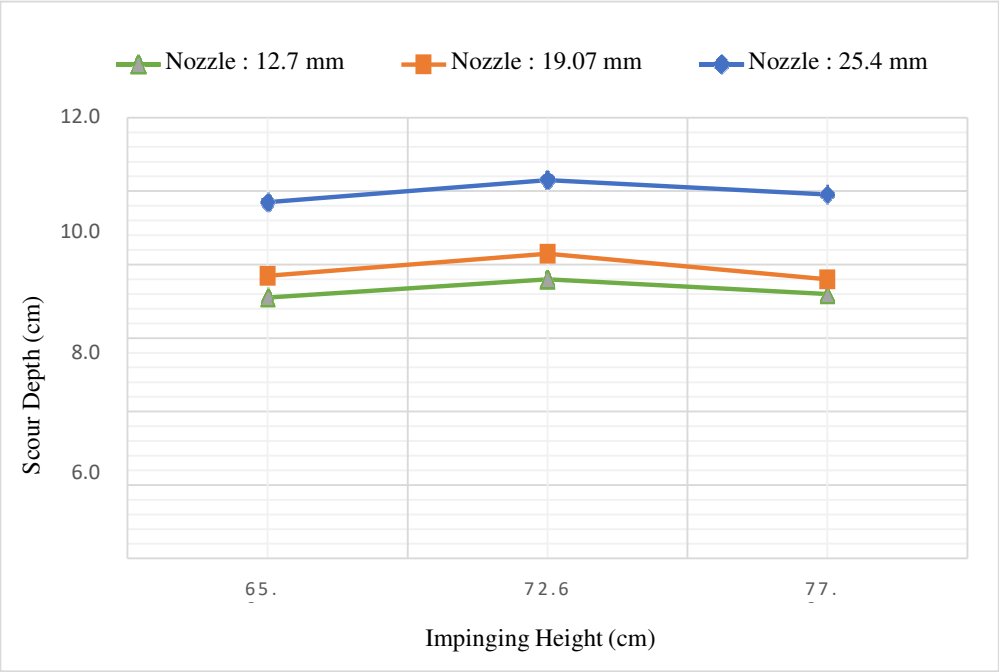

Figure 7d. Variations of scour depth with impinging height for jet velocity,vo) =3.76m/s

Effects of Jet Velocity on Maximum Depth of Static Scour

Figure 8a displays the variation of the static scour depth (ds) with the jet velocity (vo) at a fixed impinging height (hj) of 65.6 cm for nozzle diameters of 25.4 mm, 19.07 mm, and 12.7 mm of each vertical jet. This becomes clear from Figure 8a: the scour depth (ds) increases as the jet velocity (vo) increases. Improvement in nozzle diameter also results in an increase in the value of scour depth at constant impinging height.

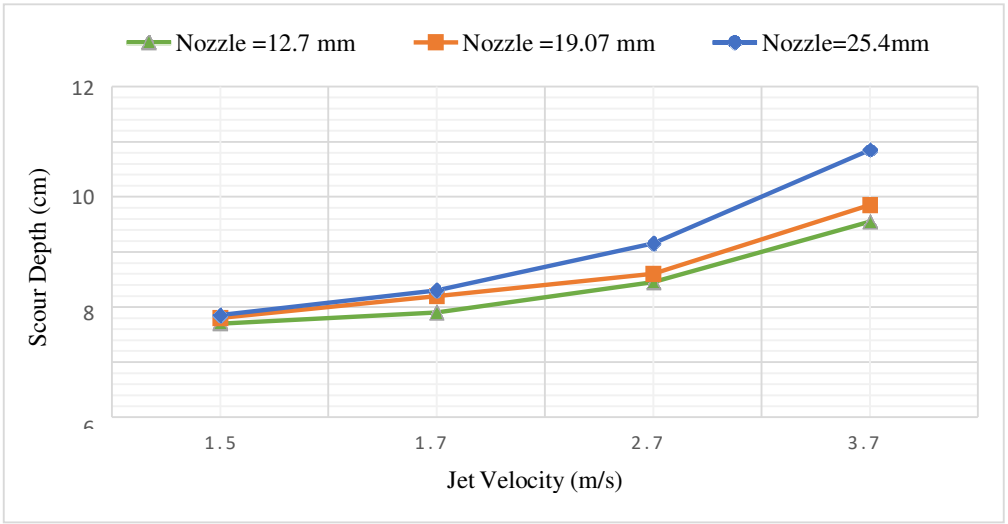

Figure 8a. Variations of scour depth with jet velocity for impinging height,(hj)=65.6cm

Similar pattern has been observed in jet diameter 19.07mm and 25.4 mm also similarly after impinging height 72.6 and 77.6 cm, the graph figure 8(b) and figure 8(c) are plotted and sametrend of results has been observed.

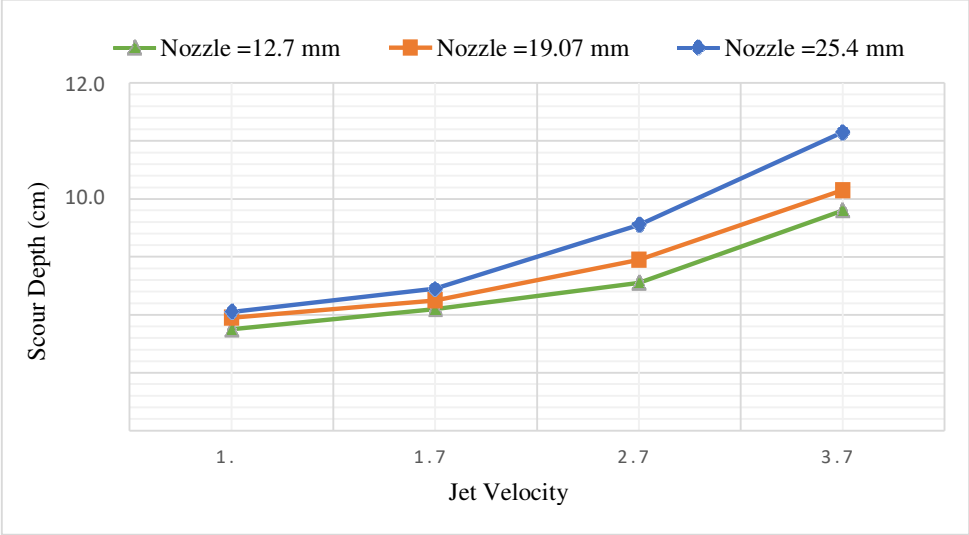

Figure 8b. Variations of scour depth with jet velocity for impinging height,(hj)=72.6cm

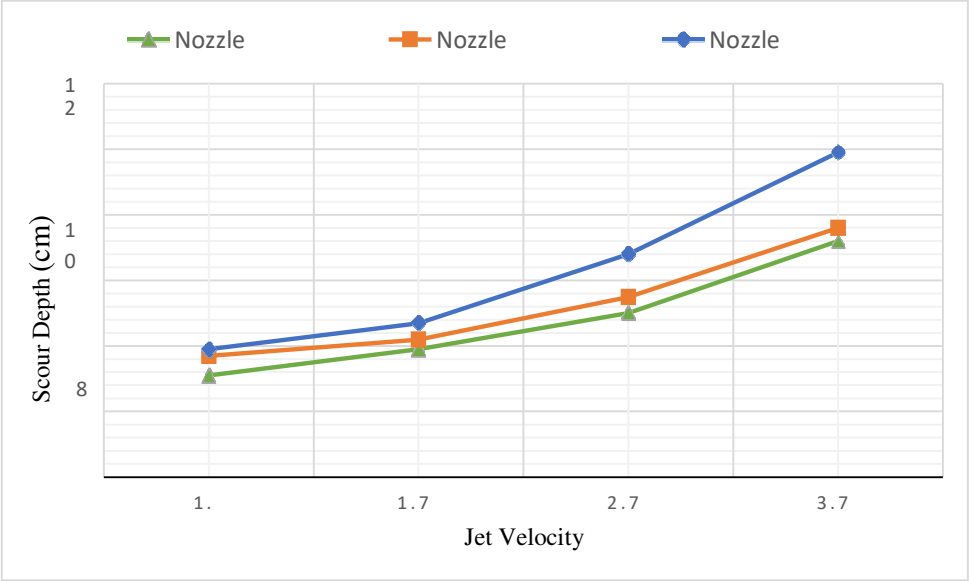

Figure 8c. Variations of scour depth with jet velocity for impinging height,(*hj*)=77.6cm

SURFER Software Used to Visualize the Soil Surface:

Golden Program, Inc.'s SURFER program is used to observe the soil surface and generate isoline maps, 3D maps, and surface areas. An algorithm is used by the computer to transform input data, which is usually measured XYZ coordinates of points, into a 3D representation that looks like a map. A regular grid of points known as the GRID is utilized to prepare XYZ data inputs for display. The GRID's primary objective is to create a surface on which the input points are evenly distributed across the XYZ points. Several features may be seen on the contour map of scour holes, including a more gradual upstream slope, a steep and protracted downstream side slope, and a characteristic scour profile shape for different velocity values. The scour holes have a parabolic shape, with the maximum depth found near the nozzle's apex.

The velocity of the jet causes the dune height, scour hole volume, and maximum depth to increase. For a given nozzle diameter and velocity, the dune height, volume, and scour hole depth all increase. The nozzle velocity and diameter grow at the same rate for the scour hole's depth, volume, and dune height.

Estimation of Various Scour Parameters

The results of a few researchers are compared with the experimental investigation being conducted now, including Westrich and Kobus (1973), Rajaratnam (1981), Aderibigbe and Rajaratnam (1996), and Ansari et al. (2003). Several equations combining scour characteristics have been provided using the collected data. These include maximum static scour depth, radius of scour hole, height of dune, and volume of scour hole.

Maximum Scour Depth

The erosion parameter, or non-dimensional parameter (EC), is defined by equation (1). Sarma (1967), Westrich and Kobus (1973), Rajaratnam (1982), Aderibigbe and Rajaratnam (1996), and Ansari et al. (2003) were among the authors who used this terminology. This equation was used to calculate Ec for the present dataset.

$$E_C = u_o(d_o/h_j)/\sqrt{g\ d_{50}(\Delta\rho s/\rho_f)}$$

Where, $(do/hj > 8.3)$ (1)

Aderibigbe and Rajaratnam (1996) derived the equation that involves the Ec for the static maximum scour depth.

$$\frac{d_{sms}}{h_j} = 1.26E_C^{0.11} - 1 \quad (2)$$

Ansari et al. (2003) updated the previous equation to provide the following one for predicting the maximum static scour depth:

$$\frac{d_{sms}}{h_j} = 1.30(E_c)^{0.15} - 1 \quad (3)$$

Figure 9 illustrates how the dimensionless maximum static scour depth changes with Ec for all of the data that are available from the searches outlined above. The static scour is clearly increasing as the erosion parameter is increasing. The maximum static scour depth is estimated using the following equation using the previously provided data:

$$\frac{d_{sms}}{h_j} = 0.0872E_C + 0.0229 \qquad R^2 = 0.87 \quad (4)$$

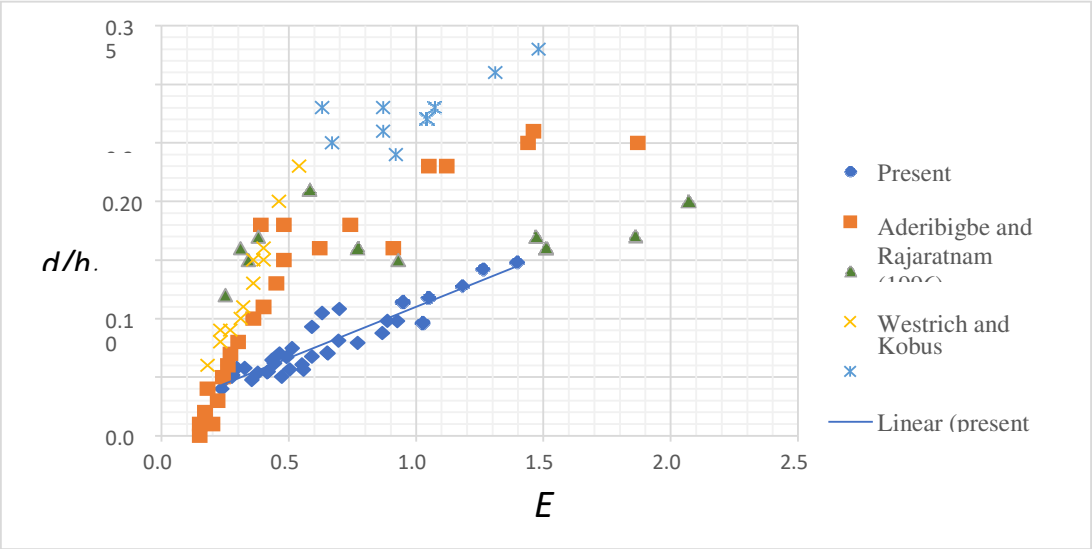

Figure 9. Disparity of dsms/ hj with Erosion Parameter (EC)

Dune Height

The change of dune height of scour was also investigated using erosion parameter for both current and past scientists' data and plotted as Figure 10. It can be seen that the dune height shows a rising tendency with increase in erosion parameter. However, the data of Clarke (1962) departed beyond the erosion parameter, *Ec* = 3. Based on the data, a following equation 5 for assessing dune height is proposed with R^2 =0.86:

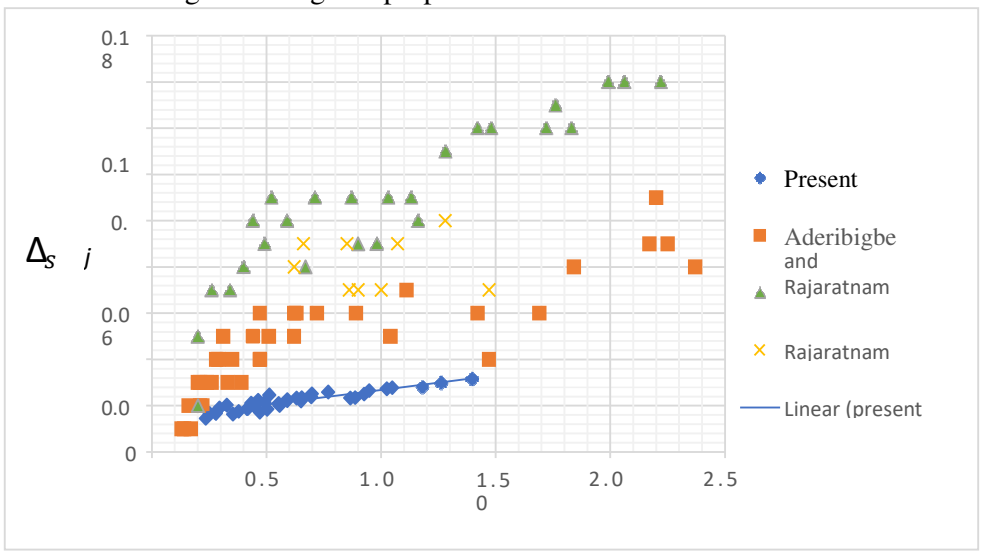

Figure 10. Variation of Δs/hj with erosion parameter (EC)

Radius of Scour Hole

The radius of scour hole change for our experimental data and the data from other researchers, Clarke (1962), Rajaratnam (1982), Aderibigbe, and Rajaratnam (1996), is shown against the erosion parameter in Figure 11. The results shown in Figure 4.8, which indicates that the radius of the scour hole increases with larger erosion parameter, are in line with the data gathered by earlier studies. Based on our data, the dune height equation (5) with R2 = 0.67 is proposed.

$$\frac{r_s}{h_j} = 0.1101E_c + 0.1439 \qquad (R^2 = 0.67) \qquad (5)$$

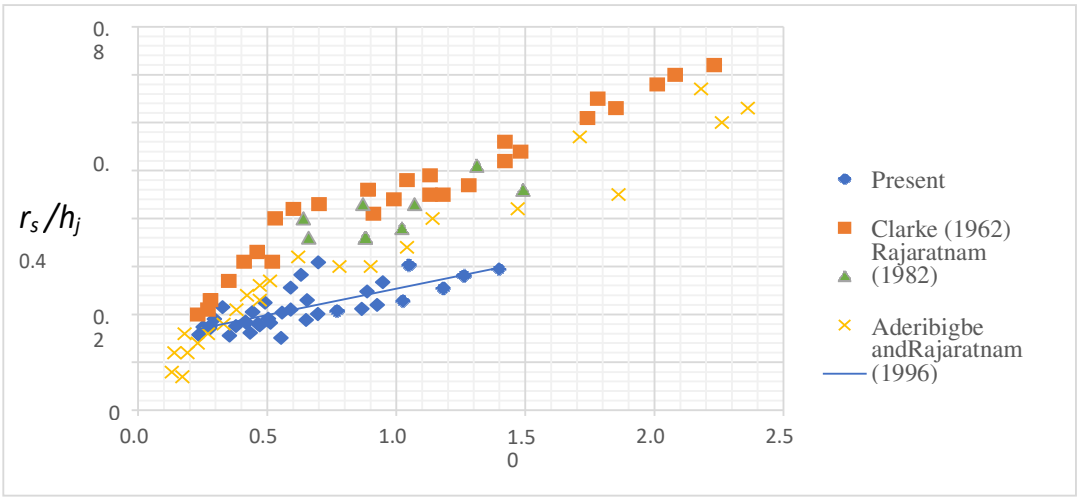

Figure 11. Variation of rs/hj with erosion parameter (EC)

Scour Hole Volume

Figure 12 displays the variation for this investigation between the scour hole volume and the erosion parameter. It is evident that the volume of the scour hole varies linearly with the erosion parameter. The scour volume increases in tandem with the nozzle diameter and jet velocity. Based on the above data, the following formula for scour hole volume with R2= 0.70 is recommended:

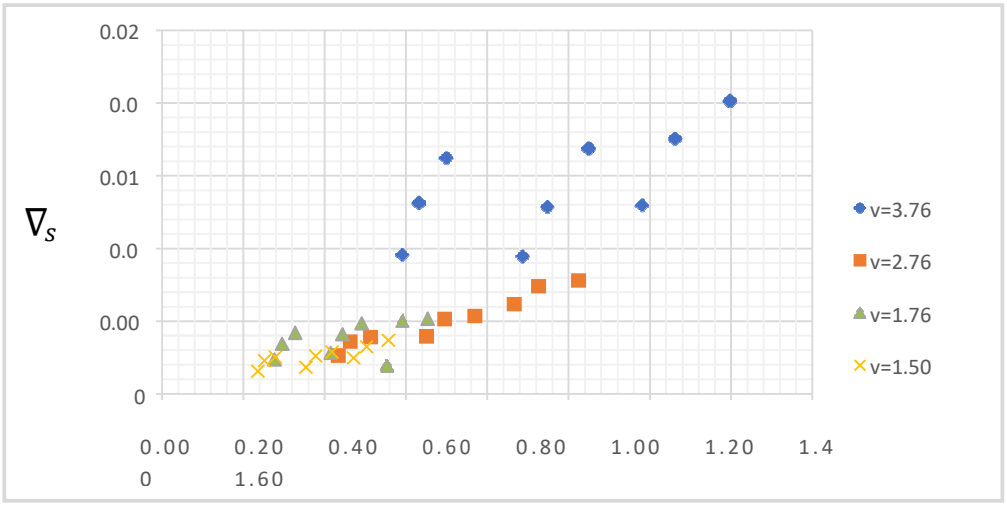

Figure 12. Variation of ∇s/hj with erosion parameter (EC)

Densimetric Froude Number

Densimetric Froude Number, a non-dimensional parameter (FD) for scour caused by a vertical jet, was used by Mazurek (2002), Rajaratnam (1981), and Mazurek & Hossain (2007). Here's how to explain it using equation (6):

$$F_D = \frac{v_o}{\sqrt{g\, d_{50} \left(\frac{\Delta \rho_s}{\rho_f}\right)}} \qquad (6)$$

Figure 13 illustrates the relationship between the Densimetric Froude number and the highest depth of scour. The following earlier studies were compared with the present research: Westrich and Kobus (1973), Rajaratnam (1981), Aderibigbe and Rajaratnam (1996), Ansari et al. (2003), and Chakravarti et al. (2014). Our data exhibits a similar trend to that of prior study, as seen in Fig. 13.

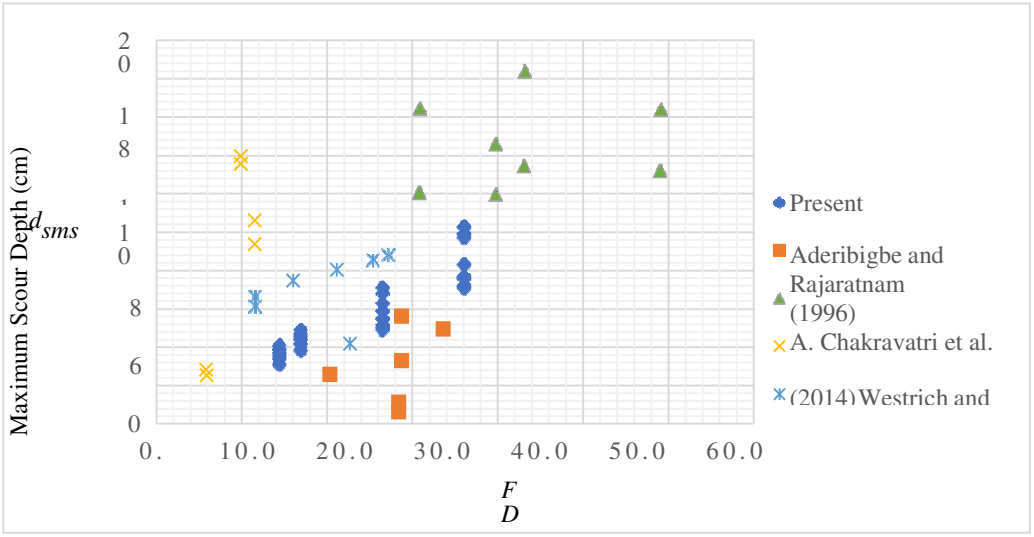

Figure 13. Variation of dsms with densimetric Froude number (FD).

Specific Energy

The specific energy involved with the jet's impact on the sediment bed is defined by equation 7 in terms of head of water:

$$E = y + \frac{v^2}{2g} \quad (7)$$

Where y = pressure head and $v^2/2g$ = the kinetic energy head.

The variation in specific energy and maximum depth of scouring are shown in Figure 13. Figure 14 illustrates how the current study's findings show a pattern that is consistent with the findings of other studies, including Chakravarti et al. (2014), Rajaratnam (1981), Aderibigbe and Rajaratnam (1996), and Westrich and Kobus (1973).

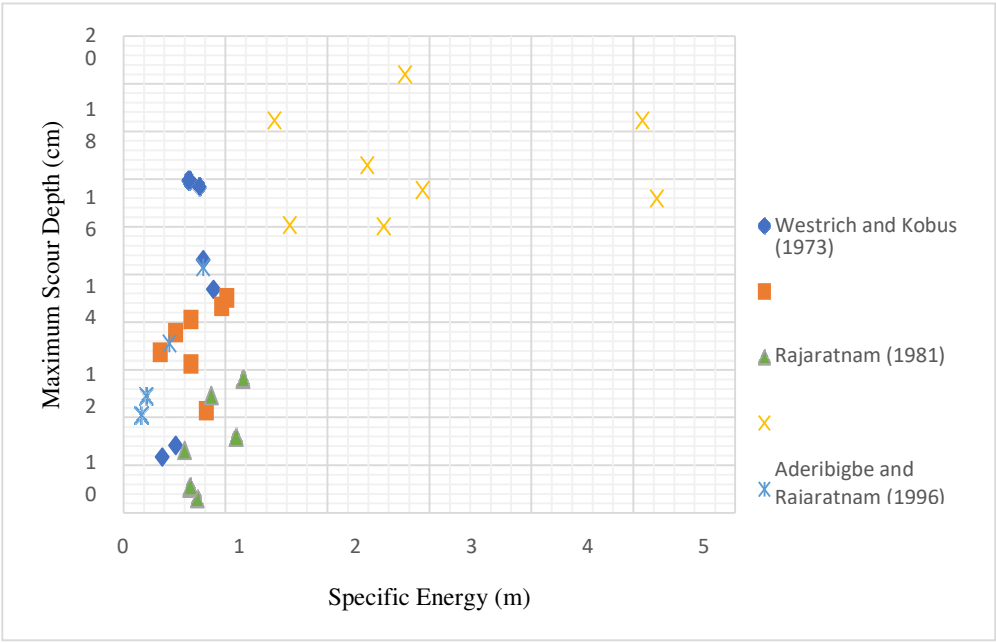

Figure 14. Variation of maximum scour depth with specific energy (E).

Impinging Height

Figure 15 displays the maximum scour depth and jet impinging height (hj) variation. Also presented for comparison are the plots from Westrich and Kobus (1973), Rajaratnam (1981), Aderibigbe and Rajaratnam (1996), and Chakravarti et al. (2014). It's possible that the study's findings revealed a clear pattern that agrees with prior findings.

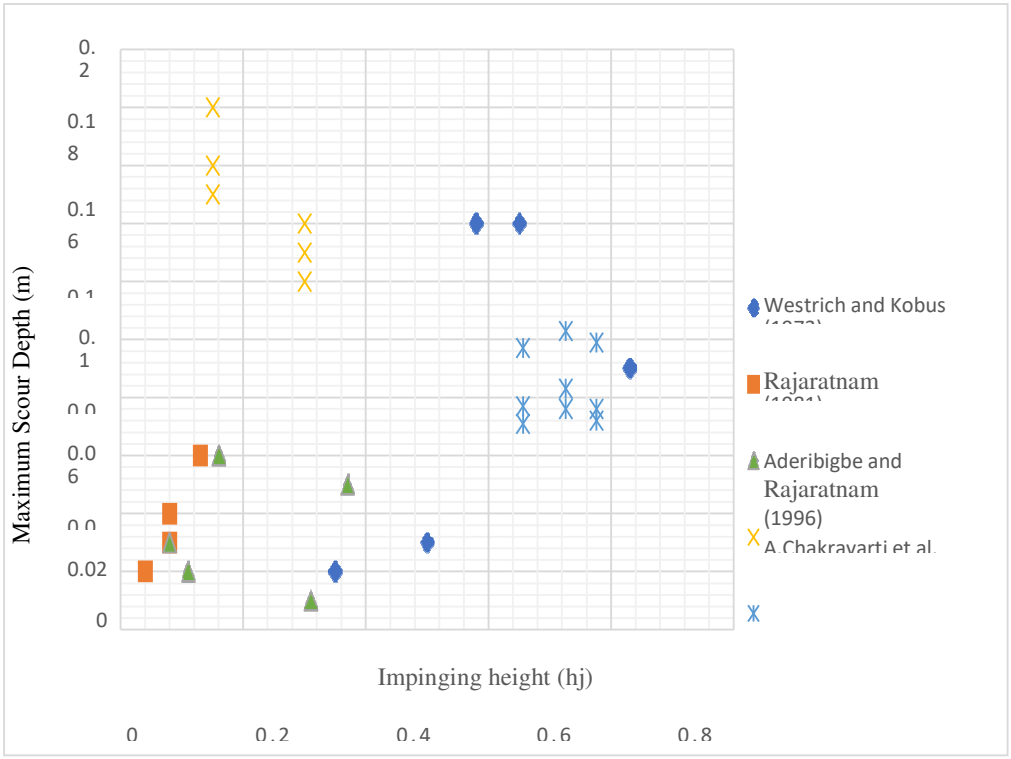

Figure 15. Variation of maximum scour depth with impinging height (hj).

Non-Dimensional Velocity

The jet's velocity (vo) may be non-dimensionalized by using the nozzle diameter (do) or the jet's impinging height. Since velocity has already been determined using the nozzle diameter. Therefore, using the jet's impinging height is more suitable in this situation. Consequently, the following is the equation (8) that was utilized to make the velocity dimensionless:

$$v_{nd} = v_o \sqrt{g h_j} \qquad (8)$$

Figure 16 displays the variation of the dimensionless velocity with the highest scour depth. The maximum scour depth is clearly increasing with dimensionless velocity. The results from Westrich and Kobus (1973), Rajaratnam (1981), Aderibigbe and Rajaratnam (1996), and Chakravarti et al. (2014) have been noted here for comparative purposes. The maximum scour depth with the dimensionless velocity exhibited a similar rising tendency, as Figure 16 shows, compared to both the current study and previous research.

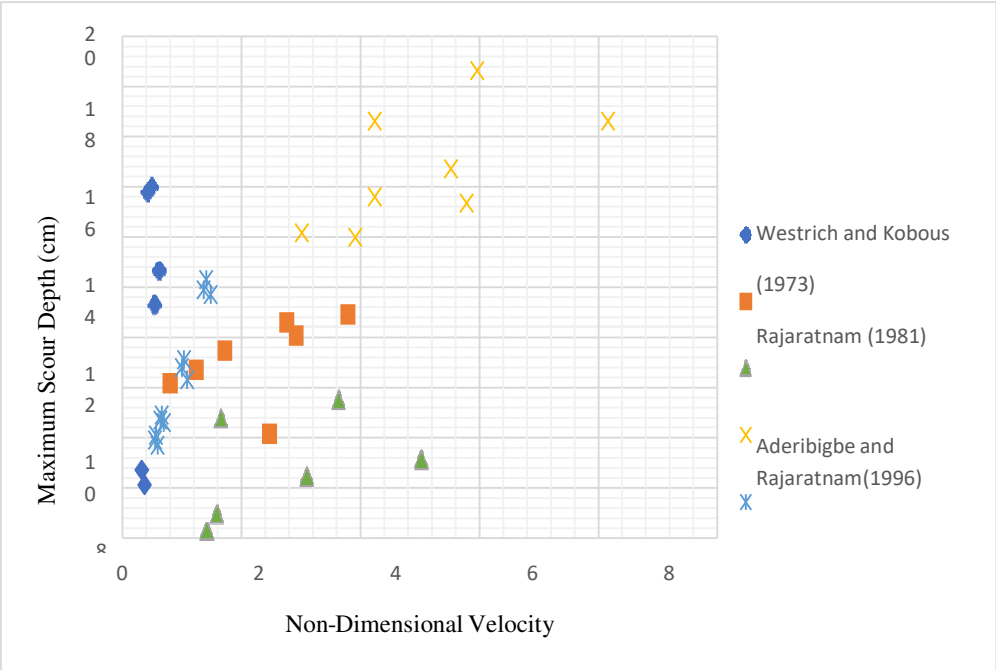

Figure 16. Variation of non-dimensional velocity with maximum scour depth

Conclusion:

Three nozzle sizes, three impinging heights, and four velocities were used in thirty-six laboratory tests to study the scour process in cohesionless silt. The results showed that although the maximum static scour depth rose with nozzle size and jet velocity, it decreased with impinging height over the critical impinging height. The kind and volume of the silt largely dictated the size of the scour hole. The nozzle diameter and jet velocity caused a rise in the scour hole's radius, dune height, and volume; however, the impinging height caused a drop in these parameters. The scour properties in cohesionless material are well described by the erosion parameters and the densmetric Froude Number. While dune formation is influenced by the kind, size, and quantity of sand present, scour hole shape is determined by sediment properties and flow patterns. It was expected that variables such as the dune's height, volume, scour hole radius, and maximum static scour depths would need to be calculated using equations.

References:

[1]. Aderibigbe O.O. and Rajaratnam N. (1996) Erosion of Loose Beds by Submerged Circular Impinging Vertical Turbulent Jets *J. Hydraul. Res.,* 34(1), 19–33.

[2]. Aderibigbe, O., & Rajaratnam, N. (1998). “Effect of Sediment Gradation on Erosion by Plane Turbulent Wall Jets.” Journal of Hydraulic Engineering, 124(10), 1034-1042.

[3]. Ansari, S. A. (1999). “Influence Of Cohesion on Local Scour.” University of Roorkee, Roorkee, India.

[4]. Ansari, S. A., Kothyari, U. C., & Raju, K. G. R. (2003). “Influence of Cohesion on Scour under Submerged Circular Vertical Jets.” Journal of hydraulic engineering, 129(12), 1014-1019.

[5]. Beltaos, S., & Rajaratnam, N. (1974). “Impinging Circular Turbulent Jets.” Journal of the hydraulics division, 100(10), 1313-1328.

[6]. Chakravarti, A., Jain, R. K., & Kothyari, U. C. (2014). “Scour Under Submerged Circular Vertical Jets in Cohesionless Sediments.” ISH Journal of Hydraulic Engineering, 20(1), 32-37.

[7]. Clarke, F. R. W. (1962). “The Action of Submerged Jets on Moveable Material,” Ph. D. Thesis, Imperial College, London, U. K.

[8]. Dey, S. and Raikar, R.V (2007). “Scour Below a High Vertical Drop.” *J. Hydraul.Eng.,* 2007, 133(5): 564-568.

[9].Doddiah, D., Albertson, M. L., & Thomas, R. K. (1953). “Scour From Jets” (Doctoral dissertation, Colorado State University. Libraries).

[10]. Dong, C., Yu, G., Zhang, H., & Zhang, M. (2020). “Scouring By Submerged Steady Water Jet Vertically Impinging on A Cohesive Bed.” Ocean Engineering, 196, 106781.

[11]. George L.R. (1980). “Impinging Jets” *Hydraulics Branch Division of Research*, *Engineering Centre Denver, Colorado,* REC-ERC-80-8.

[12]. Ghodsian M., M. M., and H.R. Ranjbar (2012). “Local Scour Due to Free FallJets in Non-Uniform Sediment.” *Vol.*19. *J. Scient.*2012.10.008.

[13]. Kartal, V., & Emiroglu, M. E. (2021). “Local Scour Due to Water Jet from aNozzle with Plates”. Acta Geophysica, 69(1), 95-112.

[14]. Litwin, U., Pijanowski, J. M., Szeptalin, A., & Zygmunt, M. (2013). Application of SURFER software in densiification of Digital Terrain Model (DTM) grid with the use of scattered points. Geomatics, Landmanagement and Landscape.

[15]. Mazurek, K. A., & Hossain, T. (2007). “Scour By Jets in Cohesionless andCohesive Soils.” Canadian journal of civil engineering, 34(6), 744-751.

[16]. Mazurek, K. A., Christison, K., & Rajaratnam, N. (2002). “Turbulent Sand Jets in Water.” Journal of Hydraulic Research, 40(4), 527-530.

[17]. Mazurek, K. A., Rajaratnam, N., & Sego, D. C. (2001). “Scour of Cohesive Soil by Submerged Circular Turbulent Impinging Jets.” Journal of hydraulic engineering, 127(7), 598-606.

[18]. Mazurek, K. A., Rajaratnam, N., & Sego, D. C. (2003). “Scour of a Cohesive Soilby Submerged Plane Turbulent Wall Jets.” Journal of hydraulic research, 41(2), 195-206.

[19]. Rajaratnam, N. (1981). “Erosion By Plane Turbulent Jets.” Journal of hydraulic Research, 19(4), 339-358.

[20]. Rajaratnam, N., and Mazurek, K.A. (2003). “Erosion Of Sand by Circular Impinging Water Jets with Small Tail Water.” *Journal of Hydraulic Engineering, ASCE, Vol.* 129(3), pp 225–229.

[21]. Rouse, H. (1940). “Criteria For Similarity in The Transportation of Sediment.” University of Iowa Studies in Engineering, 20, 33-49.

[22]. Sarma, K. V. N. (1967). “Study of Scour Phenomenon and Functional Form” (Doctoral dissertation, Indian Inst. of Science).

[23]. Shakya, R., Singh, M., Sarda, V. K., & Kumar, N. (2022). “Scour Depth Forecast Modeling Caused by Submerged Vertical Impinging Circular Jet: A Comparative Study between ANN and MNLR.” *Sustainable Water Resources Management*, *8*(2), 1-10.

[24]. Shayan M. and Fiorotto, V. (2019). “Scour Due to A Falling Plane Jet: A Comprehensive Approach.” *J. Hydraul. Eng.,* 2019, 145(4): 04019008.

[25]. Surfer® from Golden Software, LLC (www.goldensoftware.com).

[26]. Westrich, B., and Kobus, H. (1973). “Erosion of a Uniform Sand Bed by Continuous and Pulsating Jets.” *Proc., 15th IAHR Congress, Istanbul, Turkey, Vol.* 1, A13.1–A13.8.